Modelling microwave cooking; theory and experiment

C.J. Budd, Centre for Nonlinear Mechanics, University of Bath, UK,
A.D.C. Hill, Airbus, UK, G. Hooper, CCFRA, UK

1 Introduction

Microwave heating is an essential technique for cooking a wide variety of foodstuffs in both domestic and commercial applications. However, the simulation of this process remains problematic because of the complexity of both calculating a varying electromagnetic field and also determining how this interacts with the foodstuff (which is typically a complex multi-phase material). In one-dimension models have been employed to investigate moisture movement and moisture dependent parameters with **??**, **??**, [**?**] examining the use of the Lambert law approximation to the electric field. In two-dimensions models have been employed to investigate thermal runaway through phase changes and temperature dependent parameters in Nylon **??**. and a paper by Zeng and Fahgri **??** extends Lambert's law to two dimensions to investigate heating effects inside cylindrical samples of food . In three dimensions complex numerical simulations have been employed to investigate standing wave patterns set up in the microwave cavity. For example Metaxas [] has investigated the changing field patterns in turntable microwave ovens and the research team at the University of Greenwich has coupled full three dimensional calculations of the electromagnetic field with CFD calculations for the heat and moisture transport with a phase change from solid to liquid [],[]. This simulation also considers the changing dielectric properties of the food arising from heating and phase changes. Such complex calculations necessarily take a long time (typically hours or longer), even on fast computers, making fully three dimensional based computations of the microwave cooking process cumbersome to use for design calculations. A significant conclusion of the three dimensional field simulations is that they reveal that the fields in a typical microwave cavity (such as a domestic cooker) are *very* sensitive to small system variations. Thus, not only is a field calculation very expensive, if may not be particularly representative for any particular geometry. Indeed a simpler, averaged, model may give more representative solution to the problem of simultating the microwave heating of a foodstuff.

The purpose of this paper is this paper is to develop such an approximation to the electromagnetic field inside a slab-sided moist foodstuff contained within a thin thermally insulating container. This approximation is then used to derive the power source term of the enthalpy equation satisfied by the foodstuff, allowing for a phase change at 100° and appropriate boundary conditions. This geometry is typical for a foodstuff used inside a microwave cooker and a scenario used for experimental testing is shown in Figure. **??**.

PICTURE OF THE COOKER

The approximation will be used to compare the heating of foodstuffs in both mode-stirred and turntable ovens with various field configurations. The slab-sided nature of foodstuff means that for much of its length we may approximate the heating of a cross-section by solving partial differential equations posed in two-dimensions. This is a significant simplification, however, the effects of corner and side heating will be built into the model to allow for a more realistic calculation. The combination of the field approximation and the simplified geometry allows us to use a numerical method with a much faster computational time (typically minutes or less on a desktop PC) than for fully three-dimensional calculations. Using this method we calculate the temperature and moisture content of a typical foodstuff (mashed potato) at different heating times in various types of microwave oven: mode-stirred ovens rated at 650W and at 1000W and similar power rated turntable ovens. The calculated results are then compared with those obtained in experiments conducted at the CCFRA [**?**]. The results show an excThe temperature is calculated at a series of spot location within the food and compared to measurements from a thermocouple. The overall moisture content of the foodstuff is determined from weighing it at different times. The results show an excellent agreement for the temperature calculations and a reasonable ageement (within 10%) for the moisture loss over the calculation time with the agreement best for the lower power-rated ovens.

The layout of the remainder of this paper is as follows. In Section 2 we give the basic simplified equations governing the microwave heating of a foodstuff. In Section 3 we describe the fast numerical method used to solve this system. In Section 4 we apply this method to calculate the tempertaute amnd moisture loss of the food stuff. In Section 5 we compare the results to experimental data obtained at CCFRA. Finally in Section 6 we draw some conclusions from this work.

2 The field equations and their aproximations

2.1 The electromagnetic field equations

A typical microwave cooker comprises a microwave source (usually a magnetron) which sets up an electromagnetic field (through an antenna or a waveguide) within the cavity and the foodstuff. This field acts as a power source internal to the foodstuff, resulting in localised heating, possibly with a phase change. Changes in the temperature, moisture and saline content of the food, as a result of this heating, alter its dielectric properties and hence, alter the electromagnetic field. To avoid 'cold spot' due to local internal minima in the field, either the foodstuff is rotated in a turntable oven, or the field is 'stirred' by a fan in a mode-stirred oven. To simulate microwave cooking completely we must thus determine the electric field, calculate the solution of the enthalpy equation with the microwave power given by this field, and also calculate the associated changes in the dielectric parameters. For a general three-dimensional cavity this is a very large task [], however, the approximations that we describe in this

paper make it much more managable. The electromagnetic field both inside and outside the foodstuff is governed by Maxwell's equations [**?**]

$$\frac{\partial \mathbf{B}}{\partial t} + \nabla \times \mathbf{E} = 0, \tag{1}$$

$$\nabla . \mathbf{D} = \rho, \tag{2}$$

$$\frac{\partial \mathbf{D}}{\partial t} - \nabla \times \mathbf{H} = -\mathbf{J}, \tag{3}$$

$$\nabla . \mathbf{B} = 0. \tag{4}$$

The above describe the electric field intensity, $\mathbf{E}$, magnetic field intensity, $\mathbf{H}$, in terms of the electric flux density, $\mathbf{D}$, magnetic flux density, $\mathbf{B}$, vector current density, $\mathbf{J}$, and a scalar charge density function ρ, in a propagating medium. In addition to the above equations in an isotropic medium with an electromagnetic wave of angular frequency ω with magnetic permeability, $\mu(\omega)$, permittivity, $\epsilon'(\omega)$ and conductivity, $\sigma(\omega)$, the following relations hold [**?**]

$$\mathbf{D} = \epsilon' \mathbf{E} \tag{5}$$

$$\mathbf{B} = \mu \mathbf{H}, \quad \mathbf{J} = \sigma \mathbf{E}. \tag{6}$$

The permittivity, ϵ' and the conductivity, σ are sensitive to many different factors. In the particular case of foodstuffs, they vary greatly with salinity and moisture content and to a lesser extent with temperature variations [**?**]. The magnetic permeability, μ, is generally taken to be the value for free space when a non magnetic medium such as food is considered. The electric and magnetic fields used in the microwave heating of food are usually time harmonic. In this case the electromagnetic wave with angular frequency ω can be expressed as a sinusoidal temporal component and a spatial component [**?**]

$$\mathbf{E}(x,t) = Re(\mathbf{E}(x)e^{-i\omega t}) \quad \mathbf{H}(x,t) = Re(\mathbf{H}(x)e^{-i\omega t}), \tag{7}$$

where Re denotes real part.

2.2 Lambert's law

In one-dimension, assuming that the changes in the dielectric properties of the foodstuff are slowly varying with respect to the rapidly changing electromagnetic field, Maxwell's equations reduce to the Helmholtz equation.

$$E_{xx} + \omega^2 \mu(\epsilon' + i\epsilon'')E \equiv E_{xx} + \lambda^2 E = 0, \tag{8}$$

where

$$\lambda^2 = \omega^2 \mu \epsilon_0 \kappa^*(x). \tag{9}$$

Setting

$$\lambda = \alpha + i\beta. \tag{10}$$

yields the attenuation coefficient

$$\beta = \omega\sqrt{\mu\epsilon_0}\sqrt{\frac{\kappa'(\sqrt{1+\tan^2\delta}-1)}{2}} \tag{11}$$

where $\tan\delta = \frac{\kappa''}{\kappa'}$. The general solution of (8) for a finite medium in which $0 < x < l$ and the microwave radiation is assumed to strike the surface of the foodstuff when $x = 0$ (and the resulting temperature profiles arising from the microwave heating) have been studied in [**?**],[**?**]. The general solution comprises an oscillating electric field which varies around an exponentially decaying field for which

$$|E| = E_0 e^{-\beta x} \quad P = |E_0|^2 e^{-2\beta x} \tag{12}$$

where P is the power dissipation. The *penetration depth* δ of the field is given by $\delta = 1/\beta$. For a typical foodstuff δ is of the order of one to two centimetres. The expression (12) is called Lambert's law. The size of the oscillations of the field about the solution (12) depends upon the magnitude of the internal reflexions of the electromagnetic waves within the foodstuff. These are small provided that the foodstuff is large enough, and for a typical situation a length of more than 2cm is enough for (12) to be a good approximation.

2.3 The field within the oven cavity

More generally, a typical foodstuff in a microwave oven is exposed to the electromagnetic field set up within the oven cavity by the magnetron. These field patterns are very difficult to calculate exactly especially in an oven with a mode-stirring device. Inside such a mode-stirred oven a rotating metal vane scatters the electromagnetic wave resulting in field patterns which are difficult if not impossible to calculate exactly However, the effect of the scattering is to produce electric fields which are, when averaged over time, are spatially fairly uniform [**?**]. The scattering, although significantly changing the original field patterns, does not attenuate the field and so the power transmitted into the oven cavity remains the same. Consequently, we can make the approximation that exposing the food to the changing field over the course of heating (typically several minutes) is equivalent to exposing the top and sides of the foodstuff to a relatively uniform field imparting the overall same power to the foodstuff as a whole. In contrast in an oven (such as a turntable oven) with no mode-stirring device, and with a waveguide feed, standing wave patterns can arise in the electromagnetic field [**?**]. Further simulations and experiments into the nature of the field patterns have been conducted at the University of Greenwich [**?**] in which simulations of a cuboid sample of food exposed to an electromagnetic field fed directly from a waveguide onto the load are reported. These calculations indicate that inside the waveguide an input plane is excited in a TE_{10} mode and the amplitudes of the incident waves onto the foodstuff are given by

$$E_y^{inc} = E_0 \sin\left(\frac{\pi(x-x_0)}{W}\right)\cos(\omega t - \nu z_{k0}) \tag{13}$$

where x_0,y_0 are the coordinates of the corner of the waveguide, W is the length of the waveguide in the x direction, z_{k0} is the location of the excitation plane and ν is the wave mode number. The standing wave pattern arising can easily lead to *cold spots* in the food at nodes in the field. Although the turntable leads to some averaging between the effects of high and low field strengths on the food, it is still possible for the food to be exposed to strongly localised field patterns. An example of these is given by the thermal image presented in Figure 1. Here we see the results of an experiment conducted at CCFRA in which mashed potato has been heated in a 750W turntable oven and heated for five minutes.

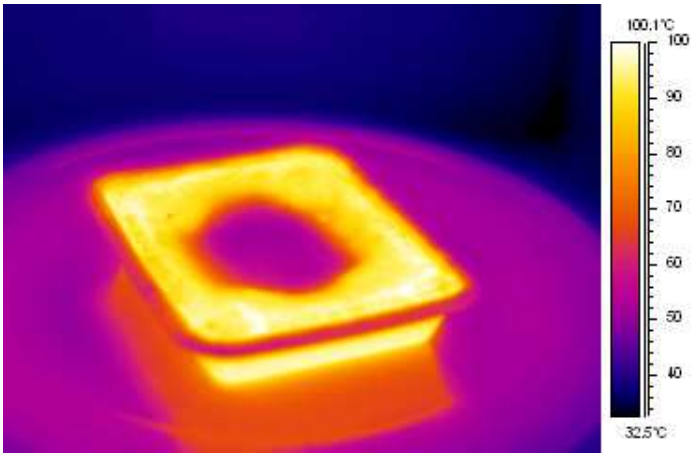

Figure 1: Thermal image of a tray of mashed potato taken after 5 minutes heating in a 750W turntable oven.

In this experiment, the foodstuff was placed at the centre of the turntable. From Figure 1 it appears that there is a minimum in the field at the centre of the oven and the food is rotated around this minimum position, accounting for the region of lower temperature evident in the thermal image. Fully three-dimensional calculations of the field are very expensive and time consuming, and for the purposes of modelling the cooking process it is appropriate to consider some approximations to the field. One quantity which can be measure accurately via experiment is the power efficiency of the oven. This is the amount of power, from that available from the magnetron, which is developed in a simple load (typically water in a simple container). Accordingly to develop a simple mathematical model for heating in a microwave oven, consistent with the above experimental results, we assume that an imposed field is applied to the *surface* of the food. This leads to an imposed surface power density, Q_0, at the boundary of the food. To do this we consider a slab-sided foodstuff which is an approximate cuboid, as illustrated in Figure **??** occupying the region

$$0 \leq x \leq L_x, \quad 0 \leq y \leq L_y \quad 0 \leq z \leq L_z$$

where y is the vertical coordinate, so that the base of the foodstuff is the plane $y = 0$ and the surface exposed to the most electromagnetic radiation is the plane $y = L_y$. Typically $L_x \approx L_z = \approx 10cm$ and $L_y \approx 2cm$.

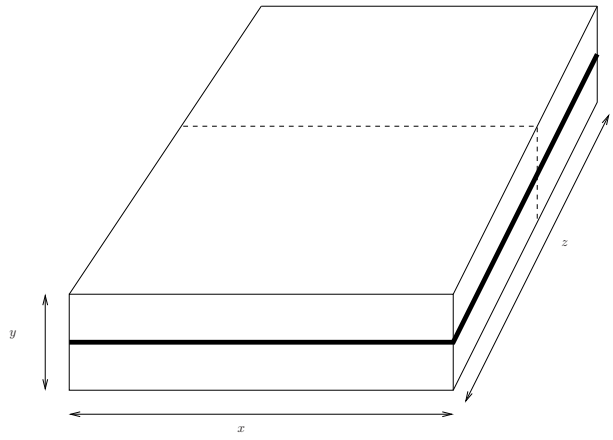

Figure 2: Schematic diagram of heated trays of mashed potato.

If we take a representative cross-section of the foodstuff at a fixed value of z then the field power density at the surface of the food can be represented by the respective functions, $a(y,z), b(y,z), c(x,z), d(x,z)$ as indicated in Figure 3

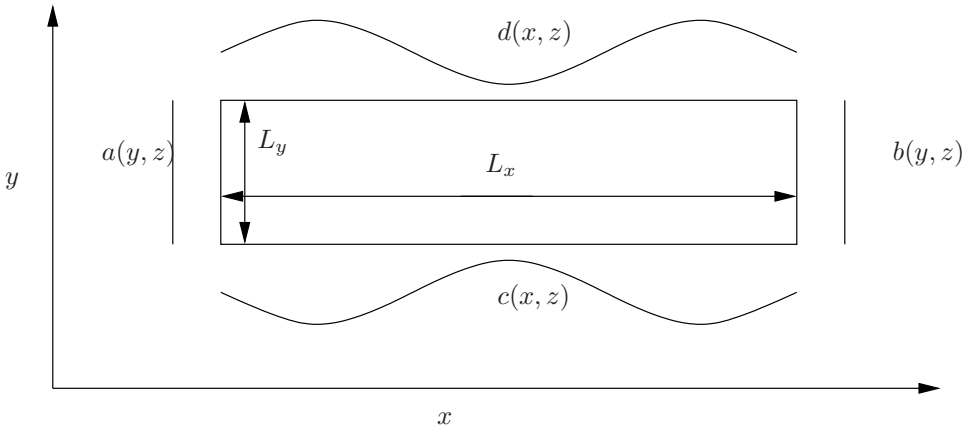

Figure 3: The geometry of the foodstuff and the surface power density functions.

In the case of a mode-stirred oven we expect that the surface field will be approximately uniform and consequently functions a, b, c, d will be essentially independent of x, y and z. In Section 5 we consider two possible situations, one where there is a significant field on the base of the foodstuff, for which $a = b = c = d$ and the second where we consider a situation with negligable

field at the base, so that $d = 0$. The latter model gives rather better agreement with the experimental results reported in Section 5.
In contrast, in the case of a turntable oven the uniform field assumption breaks down and must be replaced by a variable surface field. It is assumed that there is little variation in the field from the sides and so in (**??**) we choose $a(y) = b(y) = Q_0$. However following (13), as the surface power density power P is proportional to $|\mathbf{E}|^2$ we have

$$P_a \propto \sin^2\left(\frac{\pi(x - x_0)}{W}\right). \tag{14}$$

Accordingly we take the power density on the top surface of the foodstuff to be

$$c(x, z) = Q_0 \sin^2\left(\frac{\pi(x - x_0)}{W}\right) \sin^2\left(\frac{\pi(z - z_0)}{W}\right), \quad d = 0 \tag{15}$$

This approximation allows us to model the effects of hot and cold spots in the food without solving Maxwell's equations explicitly, although the model is not able to predict the presence of hot and cold spots a-priori.

2.4 The penetration of the field into the foodstuff

We now consider a cross-section of the slab-sided foodstuff in a rectangular tray, taken sufficiently far from the ends so that it is reasonable to use a two-dimensional approximation for the field. In Figure 4 we see a thermal image taken through such a cross section in a turntable oven.

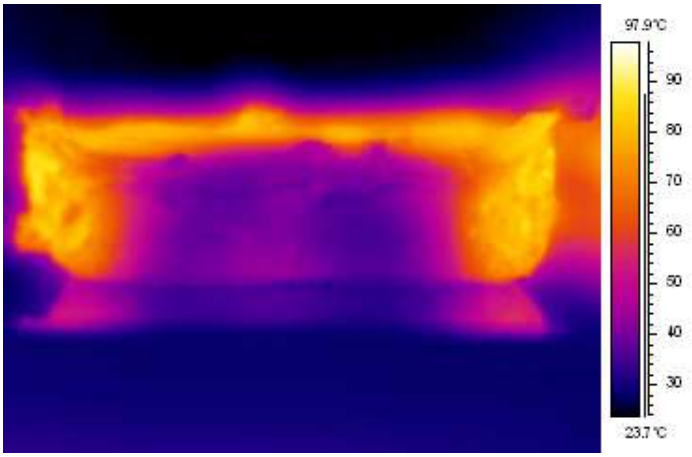

Figure 4: The thermal cross section of a sample of mashed potato after 3 minutes heating in a turntable microwave oven.

It is plain from this figure that the contours of the temperature distribution interior to the foodstuff are strongly aligned with the coordinate directions parallel

to the sides of the foodstuff. Motivated by this experiment we consider approximating the field *interior* to the foodstuff as the sum of four uncorrelated (in time) fields, obtained by solving the *one-dimensional form* of Maxwell's equations in each of the coordinate directions with the power density of the field at each of the surfaces given by the functions a, b, c, d. The dimensions of a typical foodstuff are sufficiently large for us to be able to use the Lambert law approximation (12) in each of these directions. Thus (taking a time average and making the assumption of the lack of correlation of the fields) we assume that the time-averaged power density of the field within the food stuff at the point (x, y) takes the form:

$$P(x,y) = Q_0(a(y,z)e^{-2\beta x} + b(y,z)e^{-2\beta(L_x - x)} + c(x,z)e^{-2\beta y} + d(x,z)e^{-2\beta(L_y - y)}). \tag{16}$$

Here Q_0 represents the mean power density at the surface of the material being heated. Extending this approximation along the length of the food in the z direction leads to an approximation of the food in three dimensions. This assumes that the cross section is uniform along the length of the food. This results in an underestimation of the field at the ends of the sample where there is significant contribution from five faces rather than four along the midsection. In particular the corners of the three-dimensional food experience significantly higher field intensities and we will introduce a corner correction to account for this. This approximation is necessarily rather crude, especially close to the corners of the foodstuff. However, it is very easy to use and avoids a difficult three dimensional calculation. We show in this paper that this description of the field leads to predictions of the temperature and moisture loss which agree reasonably well with experiment.

2.5 Calculation of the average surface power density Q_0

To apply the formula (16) we must obtain an estimate for the mean surface power density of the electromagnetic field at the surface of the food. This value can be estimated in a particular oven from experimental data such as that given by experiments at the CCFRA by Hooper [**?**]. In these experiments a water load of equivalent weight to the foodstuff samples was heated in the microwave oven for a fixed time and the temperature rise measured over this heating period. From this absorbed power can be determined, and is typically around 70% of the power generated by the magnetron. The power absorbed by the water load is then assumed to be equal to the power absorbed by the foodstuff. The total power absorbed by the sample can be found by integrating the heating source term (16) over the volume of the food. Equating the resulting expression with the experimental value gives the unknown average surface power density. For the mode stirred oven, where the field is assumed to be uniform, the following expression for absorbed power is obtained from integrating (**??**) with $a = b = c = 1$ and with $d = 1$ or $d = 0$ and including two extra terms to allow for the field penetrating the two ends at $z = 0$ and $z = L_z$ we have

$$\int_0^{L_z}\int_0^{L_y}\int_0^{L_x} P dxdydz =$$
$$Q_0\int_0^{L_z}\int_0^{L_y}\int_0^{L_x}\left(e^{-2\beta x}+e^{-2\beta(L_x-x)}+e^{-2\beta y}+de^{-2\beta(L_y-y)}+e^{-2\beta z}+e^{-2\beta(L_z-z)}\right)dxdydz$$
$$=\frac{Q_0}{\beta}(L_yL_z[1-e^{-2\beta L_x}]+\frac{1+d}{2}L_xL_z[1-e^{-2\beta L_y}]+L_xL_y[1-e^{-2\beta L_z}]).$$

Observe that the dominant contribution to the total power is given by the L_xL_z term.
In contrast, the power absorbed for the turntable oven with a variable field on the upper and lower surface must be calculated by taking the varying field given by (15). For simplicity we consider the case where $a = b = Q_0, c(x,z) = Q_0\sin^2(\pi x/W)\sin^2(\pi z/W), d = 0$ so that in this case

$$\int_0^{L_z}\int_0^{L_y}\int_0^{L_x} P dxdydz =$$
$$Q_0\int_0^{L_z}\int_0^{L_y}\int_0^{L_x}\Big[e^{-2\beta x}+e^{-2\beta(L_x-x)}+e^{-2\beta z}+e^{-2\beta(L_z-z)}$$
$$+\sin^2(\pi x/W)\sin^2(\pi z/W)e^{-2\beta y}\Big]dxdydz$$
$$=\frac{Q_0}{\beta}\left(L_yL_z[1-e^{-2\beta L_x}]+\frac{1}{4}(L_x+\frac{W}{2\pi}\sin(\pi L_x/W))(L_z+\frac{W}{2\pi}\sin(\pi L_z/W))[1-e^{-2\beta L_y}]+L_xL_y[1-e^{-2\beta L_z}]\right)$$

3 Temperature and Moisture loss calculation

3.1 The heat and enthalphy equations

We now consider the process of heating the foodstuff by the electromagnetic field. A typical foodstuff such as mashed potato comprises 80% water. When subjected to electromagnetic energy the temperature of the foodstuff increases rapidly, with the fastest temperature rise at the corners which are subjected to the greatest amount of electromagnetic power. Some moisture is lost during this initial heating phase due to evaporation. Experiments [**?**] in which the sample is heated for a short period of time, before any part reaches boiling point, show a small weight loss of under a gram from a 300g sample. Hence by far the greatest loss of moisture occurs at $T = T_b = 100^\circ$ when the water in the foodstuff experiences a phase change, turing into steam. Experiments conducted at CCFRA using tracer dyes within the foodstuff [**?**] indicate that there is little convection within the foodstuff and that the majority of the vapour escapes rapidly into the oven cavity without further affecting the system. The water vapour is not heated by the microwave field and so does not increase in

temperature or directly influence the field. It is further assumed (consistent with the need to maintain good food quality during the cooking process) that there is sufficient moisture in the system, and the heating time is sufficiently low, such that the food does not enter a dried phase. These assumptions mean that we need not model the gas phase and can concentrate the calculation to the liquid vapourisation. As a result of these assumptions the temperature of the food can be described by the heat equation

$$c\rho T_t = \begin{cases} k\nabla^2 T + P & T < T_b \\ 0 & T \geq T_b. \end{cases} \tag{17}$$

where P_a is the local power density of the electromagnetic field given by (16). It is shown in [**?**] that an accurate and efficient numerical method for solving this system can be obtained by discretising the systems given by smoothing the transition from heating to vapourising over a narrow temperature range. This smoothing increases the computational efficiency immensely without significantly reducing the accuracy of the model and takes the form

$$c\rho T_t = \frac{1}{2}\left(1 - \tanh\left(\frac{T - T_b}{\tau}\right)\right)\left[k\nabla^2 T + P\right]. \tag{18}$$

Here τ determines the width of the phase change range and for accuracy, we must keep τ as low as possible. In [**?**] it is found that an optimal τ of 0.05 gives a good accuracy when calculating both temperatures and phase change, but within a reasonable computational time.

We now consider the boundary conditions satisfied by the temperature. The foodstuffs considered in the experiments at CCFRA are contained in thin CPET plastic containers with the top surface of the foodstuff open to the air. This plastic is virtually transparent to microwaves but acts as a weak thermal insulator. We model the temperature in the plastic using the heat equation with no source term and no phase change and we assume that the thermal properties of the plastic given by c_P, ρ_P, k_P are constant throughout the heating process. The (two-dimensional) heat equation for the temperature of the plastic container is thus given by

$$\frac{\partial T}{\partial t} = \frac{k_P}{\rho_P c_p}\left(\frac{\partial^2 T}{\partial x^2} + \frac{\partial^2 T}{\partial y^2}\right). \tag{19}$$

The effects of this insulating layer are incorporated into the model by balancing the heat flux across the food-plastic boundary so that if the left interface between the plastic and the food is at the point $x = a$ we have

$$k_p \frac{\partial T}{\partial x}(a^-) = k\frac{\partial T}{\partial x}(a^+), \tag{20}$$

with similar equations at the other interfaces. This equation determines the heat flux into the plastic from the heated food. The plastic layer and the top food layer are in contact with the air in the oven cavity at an ambient temperature T_a leading to a loss of heat through radiation and convection. At the sides of

the sample, $x = 0$ and $x = L_x$, we impose the following heat loss boundary conditions. At $x = 0$,

$$k_p \frac{\partial T}{\partial x} = h_c(T(t, 0, y) - T_a) + \sigma\epsilon(T^4(t, 0, y) - T_a^4). \tag{21}$$

At $x = L_x$,

$$k_p \frac{\partial T}{\partial x} = -h_c(T(t, L_x, y) - T_a) - \sigma\epsilon(T^4(t, L_x, y) - T_a^4). \tag{22}$$

The surface of the food is exposed to the oven cavity where heat and moisture are free to escape at this boundary. Here the heat loss is given by

$$k \frac{\partial T}{\partial y} = h_c(T(t, x, L_y) - T_a) + \sigma\epsilon(T^4(t, x, L_y) - T_a^4), \quad y = Ly. \tag{23}$$

In the experiments conducted at the CCFRA the sample loads are placed on an insulating glass surface so we impose a zero heat loss condition at $y = 0$:

$$\frac{\partial T}{\partial y} = 0 \tag{24}$$

to model the insulating effect of the surface.

3.2 Moisture loss and end corrections

A useful experimental measure is the total moisture $M(t)$ lost from the sample during heating with the primary mechanism for moisture loss through the phase chance at $T = T_b$. The length of time that each point spends at 100 °C can be used to calculate the local moisture $m(x, t)$ lost through the latent heat equation

$$m_t = \Lambda P(x, t).$$

The assumption, based upon the experimental results, that the steam is able to leave the food easily means that we do not have to model the gas transport in the food. A complicating factor in this calculation is the fact that the dielectric properties of a foodstuff depend typically on $m(x, t)$ [**?**], but calculations reported in [**?**] for a one-dimensional foodstuff indicate that this effect is not too severe. To estimate the temperature and total moisture loss during heating using a two-dimensional calculation we assume as before that the foodstuff is a cuboid and occupies the space $0 < x < L_x, 0 < y < L_y, 0 < z < L_z$. The (two-dimensional) vertical cross-section considered when calculating the temperature of the food is given by the dotted line in Figure 2. and leads to a reasonable approximation for the temperature away from the corners. However, to estimate the total moisture loss we need to take account of the full three-dimensional geometry of the foodstuff. However, this can be achieved to a reasonable degree of accuracy, by applying an *end correction* to the two-dimensional calculation and also allowing for the effect of enhanced heating at the corners. In the microwave heating process, the decay of the electric field intensity as it penetrates

the foodstuff means that the most intense heating is concentrated in a boundary layer close to the surface of the food. This follows from the two-dimensional model and can be seen in the thermal image in Figure 4. The width δ of this layer is determined by the dielectric properties of the food and the wavelength of the applied field which together govern the attenuation of the field. The two-dimensional cross-section in the $x-y$-plane gives a good approximation to the temperature distribution of the foodstuff over much of its length but will not be accurate if $|z|$ or $|L_z - z| \approx \delta$ where heating from the sides becomes important, and the field is able to penetrate from several faces. To account for this we include an end correction to the moisture calculation. This correction assumes the fields observed at the ends of the sample are similar to the fields observed at the sides of the vertical cross section and that the moisture loss from the ends is primarily confined to the boundary layer of width δ. This end correction deals with the ends of the samples but the corners are still approximated by a field from three sides, when in reality they experience a significant field from four sides leading to an underestimation of the temperature increase and moisture loss experienced at the corners. Accordingly, to determine the overall moisture loss in the cuboid, we firstly find the moisture loss per unit length in the two-dimensional cross-section and multiply by $L_z - 2\delta$. An end correction is then applied by calculating the moisture loss per unit length in the region $0 < x < \delta, 0 < y < L_y$ and multiplying this by $2L_x$ to account for the moisture loss from the two ends of the sample at $z = 0$ and $z = L_z$.

ANDREW IS THIS CORRECT?

4 Numerical methods

4.1 Overview

We now present an overview of the numerical methods and schemes used to calculate the temperature and moisture content of the food during heating by solving (**??**)-(24). The model requires several input parameters relating to the dielectric and physical characteristics of the food and microwave oven, in particular the specific heat, density, thermal conductivity, dielectric loss and the dielectric constant of the food. The dimensions of the rectangular tray are also needed along with the power absorbed by an equivalent load. These values are then used to calculate the temperature distribution along a vertical cross section of the food. The temperature data is then used to calculate the moisture loss of the sample throughout the heating time. The schematic in Figure 5 describes the use of the code.

4.2 Finite differences and the heat equation

To solve the heat equation numerically we use a semi-discrete method. Assuming that the temperature has discrete values $T_{i,j}(t)$ over a regular mesh, we discretise the equation (**??**) in the spatial variables x and y using finite differences, leading

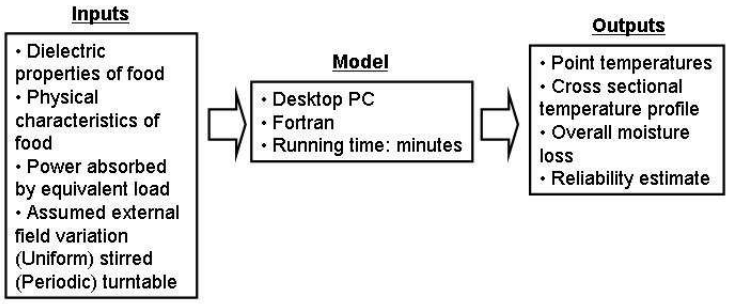

Figure 5: Diagram indicating the use of the computer code developed to solve the model for microwave heating.

to a system of ordinary differential equations for $T_{i,j}$. The heat equation is discretised at points on a two-dimensional mesh modelling the tray of food. The first five mesh points in each row in the x direction, x_1-x_5 represent the plastic boundary and are separated by a distance h_p. Similarly the final five mesh points in each row in the x direction represent the plastic and are also separated by a distance h_p between points. The points x_5 and x_{N_x-4} lie on the food-plastic interface. Inside the food the mesh points are equally spaced in the x direction with mesh spacing, h_x and a uniform spacing of h_y in the y direction. A standard central difference discretisation of the Laplacian operator gives the following discretisation of the smoothed heat/enthalphy equation (18)

$$c\rho T_t = \frac{1}{2}\left(1 - \tanh\left(\frac{T - T_b}{\tau}\right)\right)\left[k\left(\frac{\delta_x^2 T}{h_x^2} + \frac{\delta_y^2 T}{h_y^2}\right) + P(x,y)\right] \qquad (25)$$

Here $P(x,y)$ represents the heating function at the point (x,y). The boundary conditions all contain terms involving the heat flux over the interfaces of the food, plastic and air and are discretised to become the following algebraic equations. At the lower boundary $y = 0$ the condition (24) becomes

$$T(t,x,y_2) - T(t,x,y_1) = 0 \qquad (26)$$

At the left-hand plastic boundary, $x = 0$, we have the following heat loss condition

$$k_p\left(\frac{T(t,x_2,y)-T(t,x_1,y)}{h_p}\right)=h_c(T(t,x_1,y)-T_a)+\sigma\epsilon(T^4(t,x_1,y)-T_a^4). \quad (27)$$

At the right hand plastic boundary, $x = L_x$, we impose the heat flux on the outward normal

$$k_p\left(\frac{T(t,x_{N_x},y)-T(t,x_{N_x-1},y)}{h_p}\right)=-h_c(T(t,x_{N_x},y)-T_a)-\sigma\epsilon(T^4(t,x_{N_x},y)-T_a^4). \quad (28)$$

At the upper food surface, $y = L_y$, exposed to the oven cavity we impose a similar condition

$$k\left(\frac{T(t,x,y_{N_y})-T(t,x,y_{N_y-1})}{h_y}\right)=h_c(T(t,x,y_{N_y})-T_a)+\sigma\epsilon(T^4(t,x,y_{N_y})-T_a^4). \quad (29)$$

The interphase condition between the plastic and food is discretised balancing the heat flux across the interface located at x_5,

$$k\left(\frac{T(t,x_6,y)-T(t,x_5,y)}{h_x}\right)=k_p\left(\frac{T(t,x_5,y)-T(t,x_4,y)}{h_p}\right), \quad (30)$$

and at the right-hand food/plastic interface at x_{N-4}we have

$$k_p\left(\frac{T(t,x_{N_x-3},y)-T(t,x_{N_x-4},y)}{h_x}\right)=k\left(\frac{T(t,x_{N_x-4},y)-T(t,x_{N_x-5},y)}{h_p}\right). \quad (31)$$

Whearas the discretised heat equation leads to a set of ordinary differential equations in the terms $T_{i,j}$ the inclusion of the boundary conditions results in a complete set of differential algebraic equations. Furthermore, the heat equation evolves on two different timescales, the short heating timescale where the food heats up rapidly and the long diffusive timescale where heat is transported via conduction. The large difference in the two timescales and the effects of the above discretisation results in a stiff system of differential equations. Accordingly, we solve the resulting system using a stiff differential algebraic equation solver. The `Fortran` code `DDASSL` [**?**] (based on a variable order BDF method) has worked well for all calculations.

4.3 Parameter values

For all numerical calculations we chose a mesh size, h_x and h_y, inside the food of $1mm$ which was significantly smaller than the attenuation length δ. The choice of this mesh size is a compromise between the accuracy and efficiency of the computation. Figure 6 shows the moisture lost for a sample heated in a 1000W turntable microwave oven for 5 minutes calculated using mesh size of $1mm$ and $0.5mm$. We found that halving the mesh size results in a relatively small 4% increase in the calculated total moisture loss after a simulated time

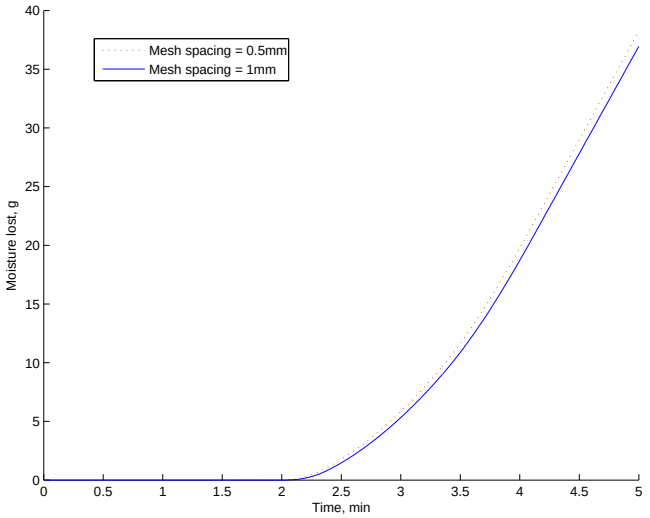

Figure 6: A comparison of the moisture lost from a sample heated in a 1000W microwave oven using mesh spacing of $1mm$ and $0.5mm$ inside the food

of $t = 5minutes$ heating. However, the the computation time (on a standard desktop Pentium PC) rose sharply from 6 minutes to 80 minutes.
The physical parameters used are listed in Table 4.3

Parameter	Value
Attenuation coefficient, β	$62.9655m^{-1}$
Thermal conductivity of food, k	$0.6Wm^{-1}K^{-1}$
Specific heat of food, c	$4200Jkg^{-1}K^{-1}$
Density of food, ρ	$1070kgm^{-3}$
Thermal conductivity of plastic, k_P	$0.1Wm^{-1}K^{-1}$
Specific heat of plastic, c_P	$2000Jkg^{-1}K^{-1}$
Density of plastic, ρ_P	$1000kgm^{-3}$
Convective heat transfer coefficient, h_c	$10Wm^{-2}K^{-1}$
Radiative surface emissivity, ϵ_{rad}	0.9
Ambient temperature, T_a	20 °C
Dimensions of sample, $L \times L_y \times L_z$	$0.02\times0.1\times0.14m$
Mesh spacing in x direction, h_x	$1mm$
Mesh spacing in y direction, h_y	$1mm$
Mesh spacing in plastic, h_p	$0.25mm$

Table 1: Parameter values

5 A comparison of experimental and numerical results

5.1 Overview

To compare the predictions of the approximate model with experiment a series of investigations were conducted at the CCFRA to gather temperature and moisture loss data for microwave cooking used samples of mashed potato in rectangular CPET plastic trays of dimensions as given in Table 4.3 and thickness ??. Mashed potato was chosen as it is an easily reproducible mixture to form. More importantly it is a relatively homogeneous, malleable, material. Since the mashed potato mixture is initially dry it was possible to record the amount of water added to the mixture to give a percentage moisture content for the sample. The plastic trays used are virtually transparent to microwaves, and so do not significantly alter the absorption of the electric field by the food. Microwave ovens use a variety of combinations and configurations of turntables, mode stirrers, waveguides and antennae in an effort to homogenise the field in the oven cavity. In the experiments conducted at the, CCFRA, three ovens are used each with a different power rating, two with a mode stirrer and antennae and oven with a turntable and waveguide. In the model described in (??) we have the flexibility of approximating the field patterns by varying the coefficients $a(x), b(x)$ etc. In this section we will explore the effect of taking differerent forms of these to allow for non-uniform fields (such as in the turntable oven) and the situation of low field surface density at the base of the food sample. The calibration of the model described in the previous chapter requires the average power absorbed by the sample as an input. To get an accurate figure for the power absorbed by the sample, a simple water load test was used with mass equivalent to that of the food load, placed in the oven at room temperature. After a set time of heating the temperature rise in the water load was measured. From the heating time and the temperature rise we could deduce the power absorbed by the water load. This value was then used to calculate the surface power density, Q_0, in the formulae (16).

5.2 The experimental set-up

The equipment at the CCFRA allowed several aspects of the heating process to be monitored. The surface temperature of the heated sample was measured using a thermal imaging camera. The thermal images produced provided a valuable insight into the variations which occur in the field inside the oven. The hot and cold spots which occur on the surface of the heated load shown in Figures 1 and 4 are evidence of the standing wave patterns set up in the oven cavity. The thermal imaging camera was unable to give an accurate temperature reading during heating as the camera could not resolve the temperature of the heated sample through the oven door. In order to gain temperature information during the heating process, fibre optic thermometry was used. Fibre optic probes in the sample allowed continuous monitoring of the temperature change at particular

points in the sample during heating. The fibre optic probes have the advantage that they have a negligible effect on the electric field inside the oven and so do not significantly affect the temperature rise. The probes were connected to a PC which recorded and plotted the temperature at each probe location at all time values. The nature of the connection to the PC meant that it was not possible to measure the temperature using a turntable oven and hence the majority of the probe measurements were made for mode-stirred ovens. As the water bound within the food is vapourised, it escapes via the surface of the food as steam. This leads to a weight loss in the sample, together with a small loss due to evaporation, which was found by recording the weight of the sample before and after heating. By heating a new sample for each run for several heating different heating times, we were able to measure the changes in the moisture content of the sample.

PICTURE OF THE SET-UP HERE

The samples used in the following experiments were Smash^{TM}instant mashed potato. The Smash is formed from a mixture of 88g dry mixture and 488g of boiling water. This is mixed until the mash forms a homogeneous consistency. The mixture is then used to fill rectangular CPET trays to a weight of 300g. This weight also corresponds to a depth of 2cm in the trays used. The surface of the samples are then smoothed to ensure an even interface. The samples are covered in a polythene film and placed in a refrigerated area overnight. The film is used to minimise any moisture lost during the chilling process. The overnight chilling process ensures that the samples are at a uniform temperature of 5°C throughout the sample. When conducting the trials the following day, the samples are collected from the chiller in small batches and kept in a domestic refrigerator in the same room as the microwave oven. The time between removing the sample from the refrigerator and heating is kept to a minimum. Once removed from the refrigerator the samples were immediately weighed, this weight was used to find the overall moisture lost during the heating process. The tray was then placed into the centre of the oven with four Fluxtron thermal probes inserted at the required location. These were held in place by means of a plastic holder in which they were threaded through small holes in the plastic and held in place (at the depth of 10mm) by rubber grommets in the configuration shown in Figure 7. The probes are separated by a distance of 20mm with probe 1 located on the food plastic boundary. The temperature at each probe was continuously recorded by the probes from a short interval before the microwave heating began to ensure that the whole heating process was captured. Once the heating regime was finished, the door of the microwave cavity was opened and a thermal image taken using a FLIR thermal imaging camera. The probes were then carefully removed and the sample weighed.

5.3 1000W mode-stirred oven

We first compare the results of our numerical calculations with the experiments conducted using a 1000W oven. The power output experiments on a 300g water

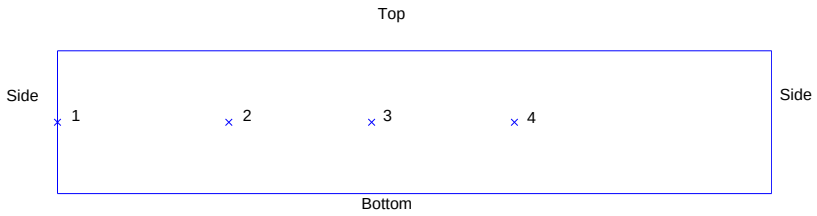

Figure 7: Probe locations in the sample.

load found an average power dump of 730W. This is used to calculate the surface power density via (17). The power rating of the oven and the power absorbed by the load have a large discrepancy of 250W. This is most likely due to uneven field effects within the oven. A thermal image of the cross section of the mashed potato after 3 minutes heating is presented in Figure 8 and we see that the heating effect inside the load is very even and confined to the top and sides. However, as a first calculation we will consider the situation where there is a uniform distribution around the surface so that $a(y,z) = b(y,z) = c(x,z) = d(x,z) = 1$ in (17).

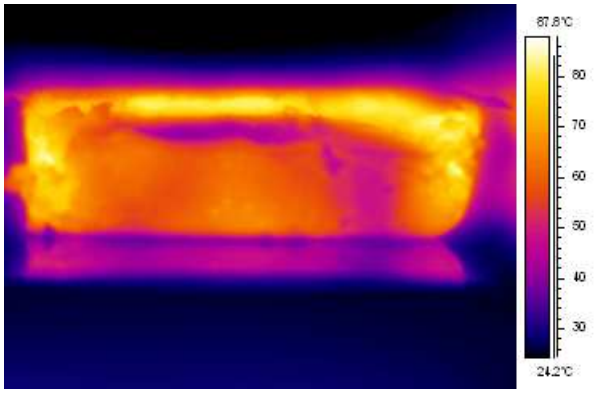

Figure 8: Thermal cross section of mashed potato heated in a microwave oven with a mode stirrer for three minutes.

Using the value for the surface power density, the model for temperature and phase change predicts the temperature profiles given in Figure 9 for 1 to 5 minutes heating.

The effects of the attenuation of the field are clear from the cross sections of the temperature distribution, the corners experience the highest field intensity which consequently leads to a higher rate of temperature increase. The edges of the sample also heat rapidly and this leads to a phase change boundary which moves into the centre of the sample. We can compare this data with the cross sectional thermal image earlier Figure 8 and also the thermal image, Figure 10,

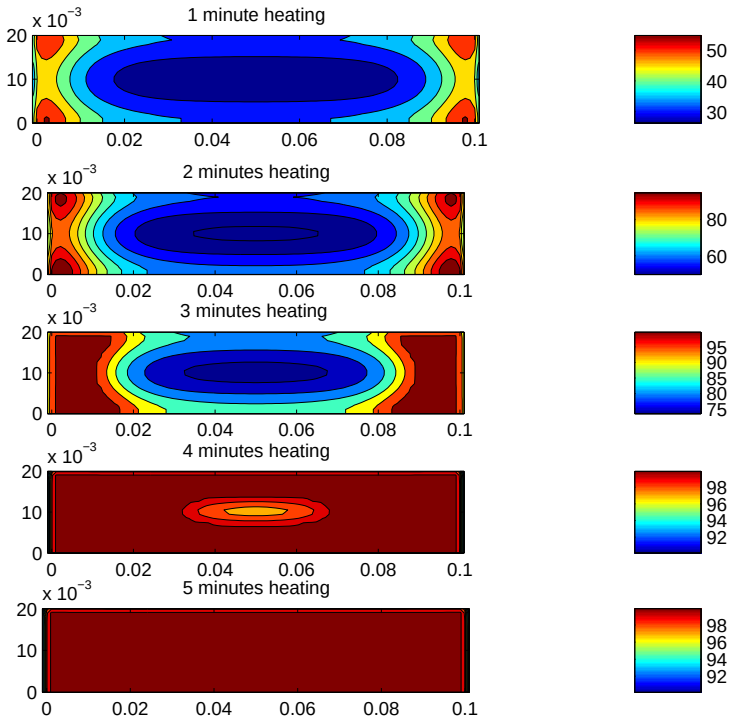

Figure 9: Contour plots of the temperature calculations in a sample of mashed potato in a 1000W oven on the assumption of uniform field penetration from all sides. Heating times are 1min, 2min, 3min, 4min and 5 minutes.

of the upper surface of the food after 5 minutes heating.

A more precise comparison can be made of the point temperatures as predicted by the model with the fibre optic thermal probe data. To make this comparison experimental data was gathered over several heating cycles and is presented as solid lines in Figure 11 with the numerical prediction for the temperature rise is given as a dashed line. In this figure we see results for the four probes. After each sample was heated the probes were removed and placed in a new sample. This made it difficult to place to probes in exactly the same position which would account for some of the variation the in the experiments. In general the agreement between the experimental and the numerical predictions of the temperature at the probes, including the point of the phase change, is good. Observe the sensitivity of the experimental results with significant variation between different experiments, but with the numerical results correctly prediction the mean behaviour. This gives confidence in the model as a good, and fast, way of predicting the temperature of the sample.

The *moisture lost* by the sample over time compared with the with the numerical prediction from the model with the end correction, is presented in Figure 12.

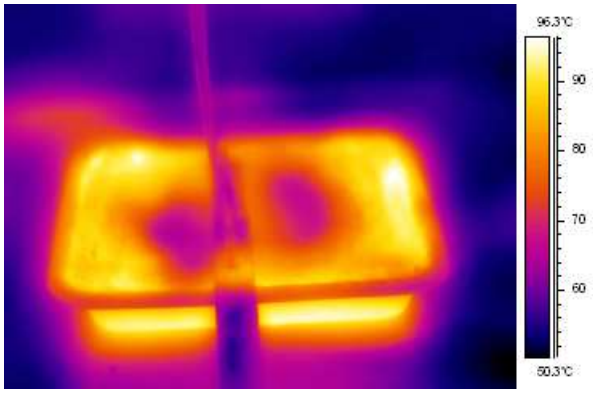

Figure 10: Thermal image of a tray of mashed potato after 5 minutes heating in a 1000W mode stirred microwave oven.The probes are visible on the top of the foodstuff

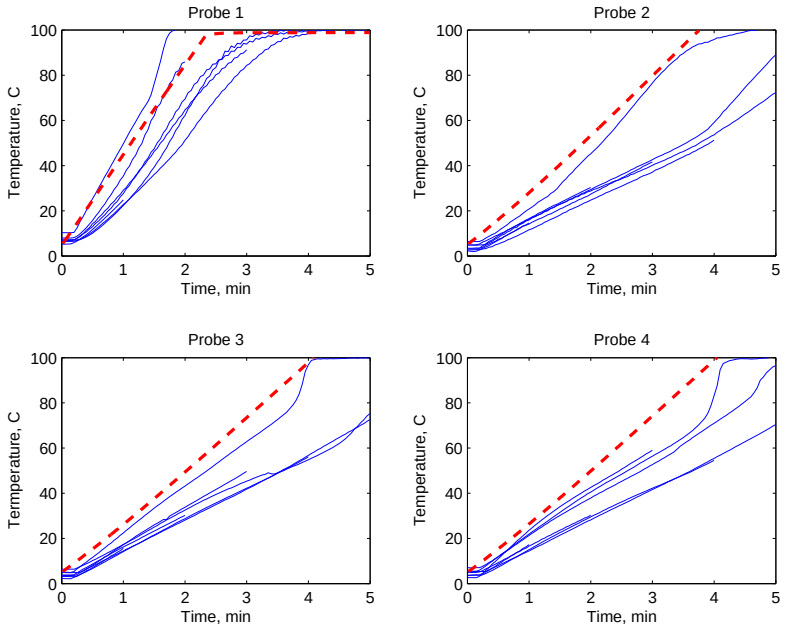

Figure 11: Comparison of experimental thermal probe data in solid lines with numerical model prediction in dashed lines for a 1000W oven.

Although the numerically computed temperature results agree reasonably well with experiment, the numerical calculation of the moisture loss, whilst of the same order as the experimental values, is a consistent underestimate. In particular, the model does not predict a significant loss of moisture until 1.5 minutes

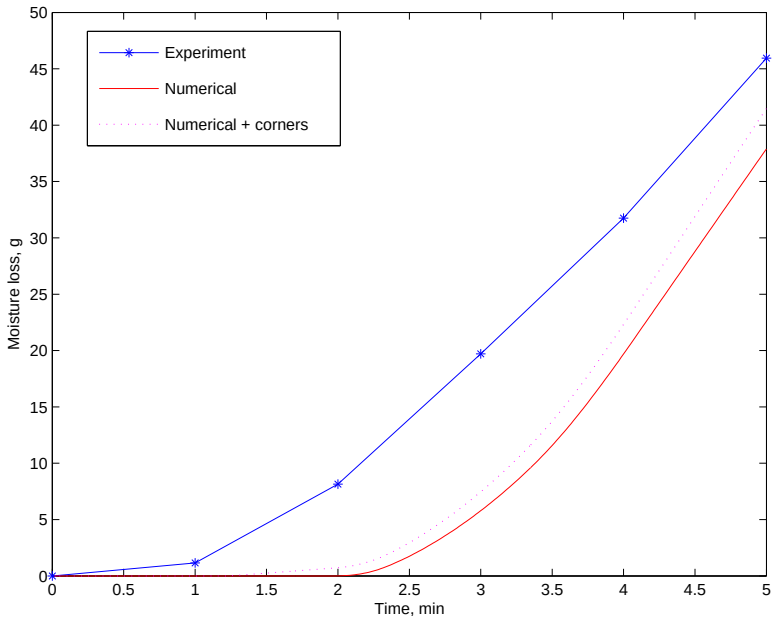

Figure 12: Moisture loss as a function of time for a 1000W oven with experimental results in solid and numerical results for the model with uniform field penetration from all sides

Heating time, min	1	2	3	4	5
Run 1	1.3g	8.5g	21g	32g	45g
Run 2	1g	7.8g	18.4g	31.5g	46.9g
Average	1.15g	8.15g	19.7g	31.75g	45.95g

Table 2: The moisture lost in each run.

after heating commences wheras the experimental data suggests that the sample begins losing moisture before 1 minute. There are two possible reasons for this. Firstly, the two-dimensional approximation to the three-dimensional geometry does not deal with the corners of the sample accurately. These are likely to be heated more rapidly than predicted by the model, leading to an earlier loss of moisture. The rate of this can be approximated by considering that of a cube irradiated from three sides of side consistent with the penetration depth. The moisture lost from a cube of volume δ^3 at each corner is calculated analytically and added on to the moisture lost predicted by the model. The dashed line represents the computed moisture loss with the effect of rapid corner heating included. The additional moisture loss improves the predicted moisture loss but the moisture lost still remains below the values observed in the experiments. Secondly, the model does not consider the initial evaporative moisture loss. al-

though it is interesting that this discrepency does not significantly alter the agreement between the temperature vaues of the predicted and experimental results.

A clear problem with the above calculation is the assumption of a uniform external field, wheras it is more likely that there is much reduced field penetration from the base of the sample. Accordingly, as a second calculation for this system, and motivated by the temperature contours presented in the experimentally obtained Figure 8 we considering the case no field penetration from the base but with the same total power is absorbed as before. This corresponds to taking $a(y,z) = b(y,z) = c(x,z) = 1, d(x,z) = 0$ in (17). Making this assumption of small power density on the base results in a higher field intensity on the remaining three faces and subsequently a higher moisture loss there. The cross sectional temperatures contours arising in this case are given in Figure 13. These show a much better correspondence with the experimental values given in Figure 8.

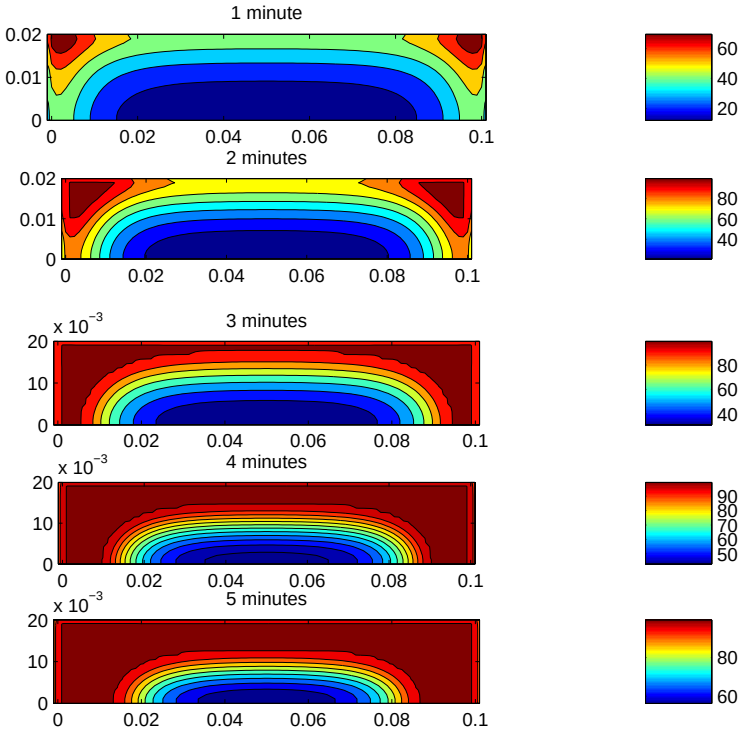

Figure 13: Contour plots of the computed temperature of a sample of mashed potato in a 1000W oven with *no field penetration from below*. Heating times are 1min, 2min, 3min, 4min and 5 minutes.

The point temperatures along the midsection do not change greatly ANDREW

DO YOU HAVE THESE FIGURES???

Finally, in Figure 14 we present the moisture loss profile from this model compared with experiment.

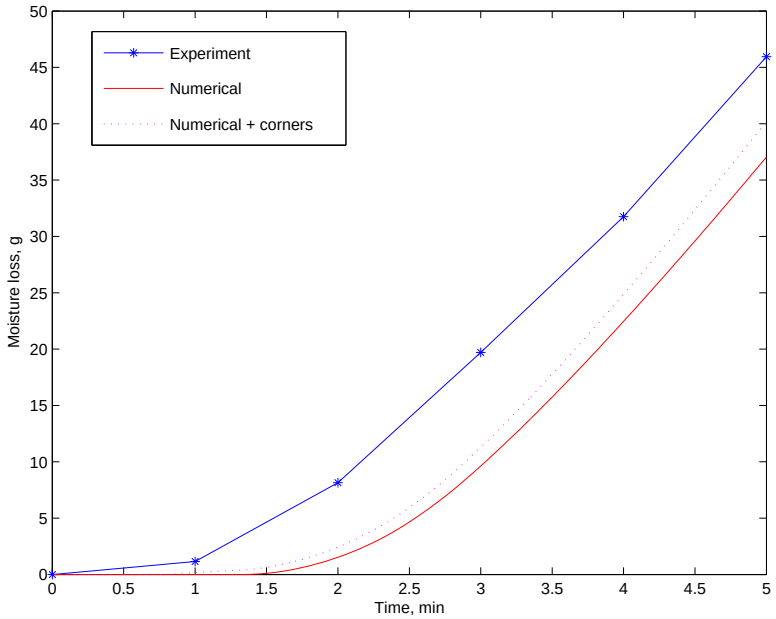

Figure 14: Moisture loss curves for a 1000W oven with no field penetration from the base.

It is apparent from this figure that the model with no field penetration from the base gives a closer approximation to the rate of moisture loss than the earlier model Indeed asymptotically the predicted and measured curves are parallel which is consistent with the assumption that there is some initial evaporative moisture loss in the early stages of heating which is not captured in the model. This closer agreement between the results above indicates that the assumption of low field penetration from below is a reasonable one, and will be adopted for further calculations. Indeed, nn practice this field intensity will be both hard to measure and to calculate due to the complicated geometry at the base of the foodstuff.

5.4 650W mode-stirred oven

We now compare the numerical results with experiments using a lower power mode-stirred oven rated at 650W. The power output experiments on a 300g water load find an average power dump of 615W so that in this case the majority of the power entering the oven cavity is absorbed by the load. This value is again used to calculate the surface power density taking a uniform field on the upper

surfaces, so that $a = b = c = 1$, and a zero field on the lower surface, so that $d = 0$. The point temperatures predicted using the mathematical model with uniform heating are compared with the fibre optic thermal probe data in Figure 15. and the contour profiles for the temperature in this case are presented in Figure 16.

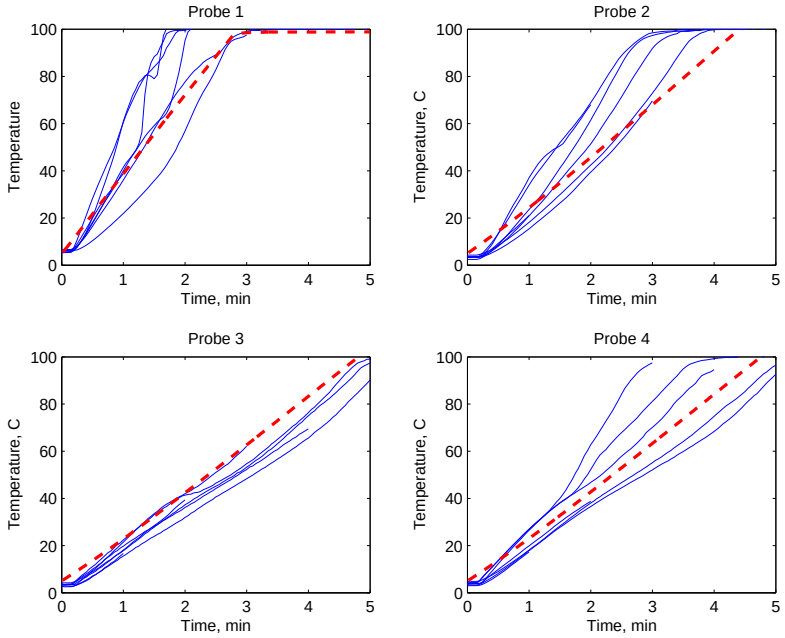

Figure 15: Comparison of the experimental thermal probe data in solid with the numerical model prediction in dashed lines for the 650W oven.

Interestingly, the numerical calculations give a closer agreement to the measured values at the probes for the 650W oven than the 1000W oven previously considered.
The moisture loss profile is presented in Figure 17. As before, the model with no heating from below gives a very reasonable agreement with the experimental values, with the two curves asymptotically parallel. As in the case of the 1000W oven, the moisture loss predicted by the model underestimates the experimental values, again possibly due to evaporative loss. However, the numerical approximation is within ?? % of the experimental value after 5 minutes heating.

5.5 750W oven turntable oven

I WANT TO RETHINK THIS SECTION. FIRSTY CAN WE REDO THE CALCULATION WITH A UNIFORM A=B=C=1 D=0 ASSUMTION TO SHOW THAT IT IS VERY WRON. THEN REPEAT IT WITH A MORE CAREFUL

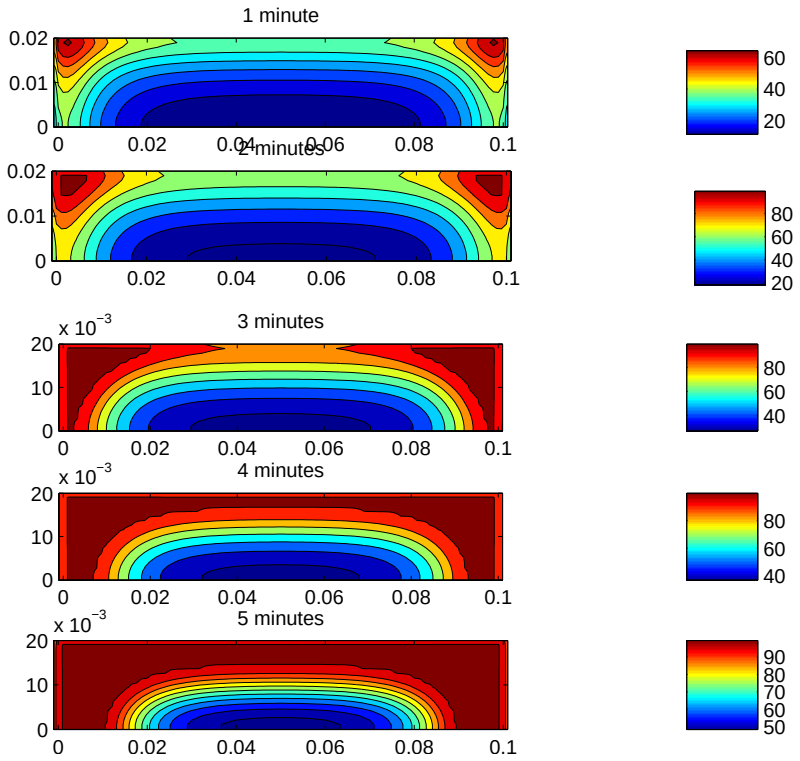

Figure 16: Contour plots of the temperature in sample of mashed potato in a 650W oven with no heating form below. Heating times are 1min, 2min, 3min, 4min and 5 minutes.

Heating time, min	1	2	3	4	5
Run 1	0.4g	3.4g	9g	18.6g	30.2g
Run 2	0.3g	2.3g	7.1g	15.2g	24g
Average	0.35g	2.85g	8.05g	16.9g	27.1g

Table 3: Moisture lost in each run.

SINUSOIDAL CALCULATION IVE WRITTEN UP WHAT I THINK HAPPENS IN THIS CASE BUT WE NEED TO DO A BIT MORE WORK HERE. We will now look at the numerical and experimental results for a 750W turntable oven. The power output experiments conducted using a 350g water load find an average power dump of 690W. The use of a turntable prohibits the use of thermal probes (as the feed wires become tangled) and so had to rely on thermal images to provide temperature information on the heated sample. As described earlier, the field in this case has significant standing wave patterns and the thermal image of samples presented in Figure 1 clearly shows the variations

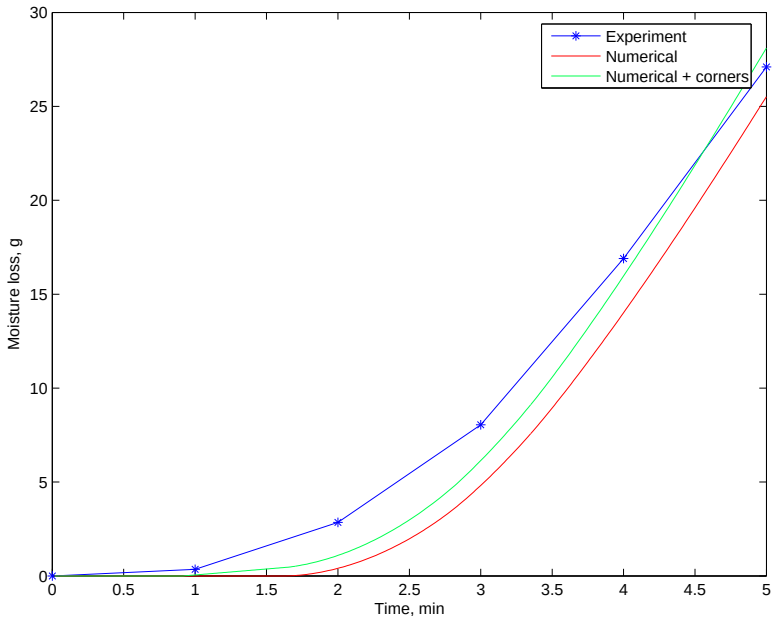

Figure 17: Moisture loss curves for a 650W oven assuming no heating from below.

in the field on the upper and lower surfaces. To compare with the previous calculation for a mode-stirred oven we initially take $a = b = c = 1$ and $d = 0$. In this case the moisture loss profile takes the form ????. The results from this calculation show ...? Clearly this is incorrect with .....

For a more representative calculation we now assume a sinusoidal variation in the field intensity on the surface of the foodstuff so that the power density $c(x, z)$ is given (**??**). The predicted cross sectional temperatures from the resulting model are given in Figure 18.

The approximation to the field patterns leads to a cool region in the centre on the upper surface. As in the previous cases, the weight of the samples before and after heating are used to estimate the moisture lost by the sample. The numerical model described above reveal the moisture loss curves as given in Figure 19.

Heating time, min	1	2	3	4	5
Run 1	0.8g	7.2g	16.2g	25.1g	39g
Run 2	0.9g	5.6g	15.9g	24.9g	37.7g
Average	0.85g	6.4g	16.05g	25g	38.35g

Table 4: Moisture lost in each run.

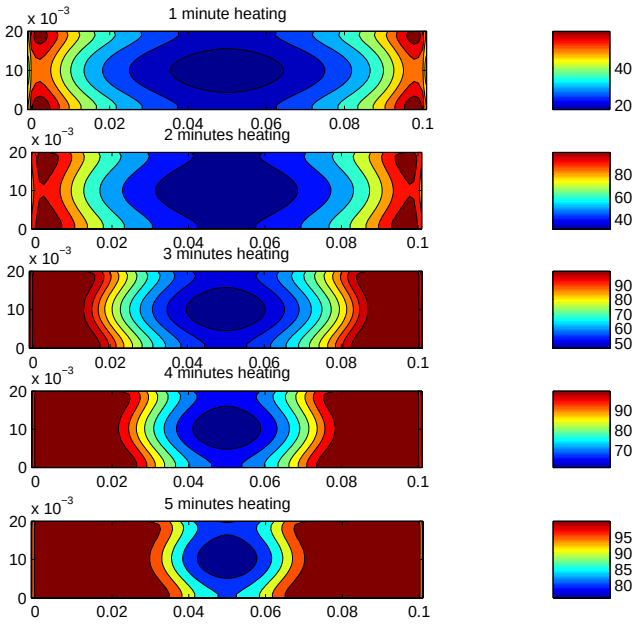

Figure 18: Contour plots of the temperature in sample of mashed potato in a 750W turntable oven. Heating times are 1min, 2min, 3min, 4min and 5 minutes.

As in the previous examples the model initially underestimates the moisture lost by the sample. The predicted rate of moisture loss is higher than the observed rate and so after 4 minutes heating the predicted moisture lost by the sample exceeds the experimental value.

NO WAY IS THIS GRAPH ANY GOOD AS IT STANDS AS IT PREDICTS THE WRONG GRADIENT. CAN WE RECALCULATE THIS.

6 Conclusion

TO BE REWORKED We have developed a simple model for the temperature evolution and the moisture loss of a sample of chilled food heated in a microwave oven. The electric field was approximated in two dimensions using the Lambert's law approximation with the surface field given by simple empirical laws. Variable fields were found to occur in turntable ovens and these were modelled by assuming an imposed sinusoidal surface power density. This variation also allowed a comparison of models with no filed penetration beneath the sample. The model was first used to calculate the temperature distribution in a vertical cross section of rectangular tray of mashed potato and then to calculate the moisture lost by the sample throughout the heating process. The moisture loss, found numerically, was found to underestimate the experimental values. This was found to be, in part, due to end and corner effects. The end effects were

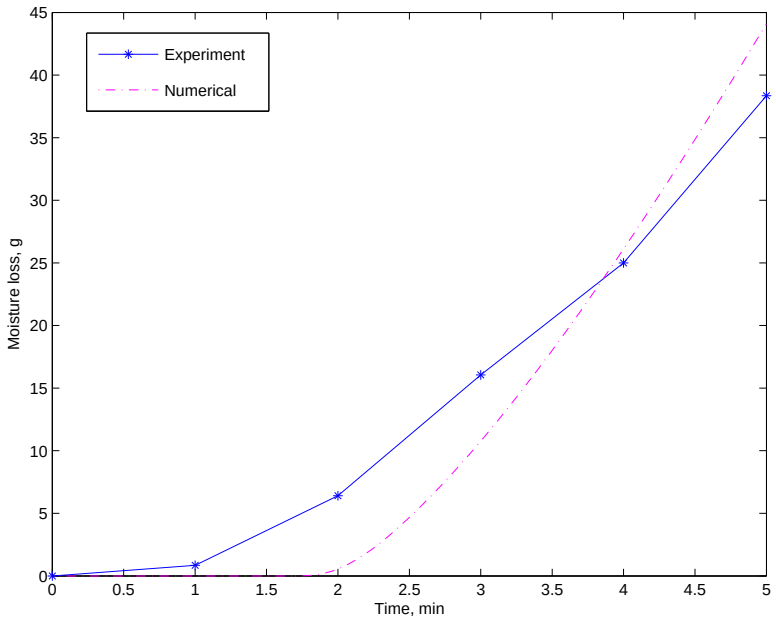

Figure 19: Moisture loss curves for the turntable oven.

incorporated into the model however the corner effects are the result of field patterns in three dimensions and were not included in the model. The power absorbed was calculated using the dielectric properties of the food.

The model appeared to agree with the experiments on samples of mashed potato in rectangular trays. The point temperatures taken midway into the sample were found to lie slightly above or in the centre of the predicted temperatures. The moisture loss was found to be sensitive to the imposed field but still gave an estimate within ??% of the moisture loss at the end of the heating time. The cross sectional temperatures appear to be consistent with the thermal images provided that a uniform field is assumed for a mode stirred oven and a sinusoidal field is assumed for the turntable oven The model has shown good average predictions in a calculation time of only a few minutes on a desktop machine.

The model was not able to calculate the moisture lost in the early stages of heating, this lead to an underestimation of the overall moisture loss. The model does not take into account evaporative losses and assumes a very simple model for moisture escape. The model is unable to predict the temperatures throughout the entire sample as corner effects become prominent and these are not included in the model in the interests of maintaining a low computation time. The calculations require an estimation of the external field to account for variations such as are seen in the turntable oven.